

Integration of wafer and plate-based NIL for scalable manufacturing of high-quality AR waveguides

Brian Bilenberg¹, Ankit Bisht¹, Vladimir Miljovic¹, Frederik Bachhuber², Christian Hellmann³, Leo Peltomaa⁴, Pekka Laiho⁴, Murat Devenci⁵, Aaron Krieg⁶, Neil Pschirer⁶, Andrea Scheidegger⁷, Erhan Ercan⁷, Mariana Ballottin⁷

NIL Technology ApS (Denmark)¹; SCHOTT AG (Germany)²; LightTrans International GmbH (Germany)³; OptoFidelity Oy (Finland)⁴; OptoFidelity Inc. (United States)⁵; Pixelligent Technologies LLC (United States)⁶; Morphotonics B.V. (Netherlands)⁷

ABSTRACT

One of the critical components of Augmented Reality (AR) glasses is the optical waveguide. Various manufacturing methods for waveguides are currently being investigated, predominantly based on the well-established wafer-based value chain. In this study, we propose an alternative approach that combines the wafer-based value chain with the high-volume, low-cost manufacturing capabilities of large-area Roll-to-Plate (R2P) Nanoimprint Lithography (NIL). This approach demonstrates the upstream and downstream process compatibility of large-area NIL. To validate this, we developed a diffractive waveguide design featuring multi-depth slanted gratings with a 25° slant angle. This design addresses the refractive index mismatch between the substrate and the nanograting resin. We utilized multiple ultra-flat high-refractive-index glass wafers ($n = 2.0$) with 200 mm diameter, paired with solvent free and solvent containing resins ($n = 1.9$). Our results showcase the scalability and quality of this method using a carrier-based imprint (Gen3 panel size, 550 mm x 650 mm), enabling the simultaneous imprinting of five 200 mm wafers, each containing four waveguides, in a single cycle.

Keywords: augmented reality, waveguides, high index resin, high index glass, nanoimprinting, large-area NIL, optical design, metrology.

1. INTRODUCTION

As a consortium, we have demonstrated the potential of large-area R2P NIL for mass manufacturing of high-quality AR waveguides. The whole manufacturing process chain has been demonstrated, from design and materials to nanoimprinting and performance testing. Surface relief gratings (SRG) with high pitch accuracy, low residual layer thickness, and high refractive index materials (up to 2.0) have been successfully replicated using large-area NIL. [1-3]

Most of the supply chain and processes around AR waveguide fabrication are currently optimized for round wafer substrates. This work highlights that large-area imprint technology can be exploited for high throughput by leveraging large-panel rectangular substrates and by imprinting multiple smaller round substrates in a single imprint cycle. This approach ensures compatibility with all up- and downstream workflows around wafer processing. Specifically, this study exemplifies scalability on a Gen3 imprint area (650 mm x 550 mm) where five 200 mm diameter round substrates can be imprinted in a single imprint cycle. This capability is demonstrated using both solvent-free and solvent-containing resins to achieve low residual layer thickness, as well as using different quality high refractive index glasses, including ultra-flat polished glass. An AR waveguide design consisting of slanted and binary gratings is used and the quality and performance of the manufactured waveguides are assessed using Littrow diffractometry and image quality measurements.

2. KEY TECHNOLOGIES

2.1 Waveguide design (LightTrans)

The design process for AR lightguides typically involves two distinct stages. First, the general layout of the lightguide is defined and optimized based on established templates, such as 1D-1D or 2D pupil expansion gratings. Second, the parameters of the employed gratings are optimized to achieve the desired optical performance.

The presented design utilizes a 1D-1D pupil expansion approach, with simulations and optimizations conducted using VirtualLab Fusion. AR waveguides based on this approach comprise three gratings: an incoupling (IC), an expansion (EPE), and an outcoupling grating (OC). Previous designs relied on blazed gratings for the incoupling and binary gratings for the expansion and outcoupling regions [1-3]. Recent advancements in imprinting technologies have enabled the integration of slanted gratings, providing increased design flexibility. In this design, slanted gratings were implemented for IC and OC, optimizing structural parameters such as height, fill factor, and slant angle to enhance system performance.

Grating orientation and period were determined during layout design. The IC and OC gratings feature a period of 400 nm, while the EPE grating uses a period of 283 nm. For parametric optimization, a linear modulation scheme was employed, varying the grating parameters along the pupil replication direction (horizontal for the expansion, vertical for the outcoupling grating). Initial investigations showed that the slant angle of the EPE grating had negligible impact on system performance - due to the significant conical incidence on this grating. Consequently, this parameter was excluded from optimization, reducing the complexity of the parameter space.

The refractive index mismatch between the substrate ($n = 2.0$) and resin ($n = 1.86$) was included as a critical design consideration. Further analysis revealed that this mismatch had negligible influence on both the grating efficiency and polarization effects. To ensure precision, the resin properties were systematically integrated into the design process through parametric optimization.

The final configuration includes a slanted IC grating (slant angle: 24.9° , fill factor: 70.5%, height: 399 nm), a binary EPE grating with variable fill factors (79.2–88.4%) and heights (38–145 nm), and a slanted OC grating (slant angle: -24.9° , fill factors: 28.2–47.4%, heights: 58–394 nm). To align with fabrication constraints, these variations were discretized into ten sections for the expansion grating and seven sections for the outcoupling grating region. A visualization of the design is provided in Figure 1.

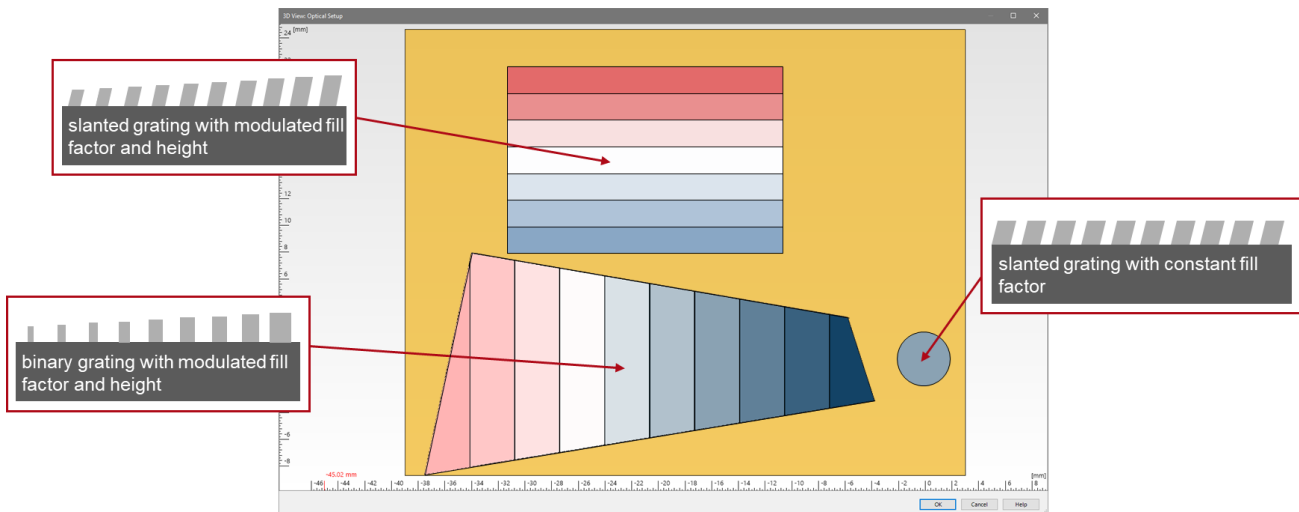


Figure 1 Resulting lightguide design with segmented grating regions and different grating types for incoupling, expansion and outcoupling gratings.

2.2 Master (NIL Technology)

One full eye-piece Surface Relief Grating (SRG) waveguide 6-inch master (Figure 2a) was fabricated on a silicon substrate tailored to optical design by LightTrans (see Section 2.1). The gratings on the master were fabricated using electron beam lithography and structures were transferred into the substrate using proprietary dry etch processes. This approach for master fabrication ensures the highest possible quality of SRGs, with electron beam lithography providing high pitch and lateral dimensions accuracy and dry etching delivering precise control of grating depths and high structure fidelity. Figure 2c shows a stitched automated microscope image of the master taken with 5X objective. Second generation replica (Figure 2b) acts as working master for further replications. Etch processes are carefully calibrated on monitor chips (gratings shown in Figure 2d – 2h), which served as test substrates to validate etch parameters. The structures on these monitor chips were characterized using SEM before etching the final master. This process allows for optimization of each of the 18 distinct gratings sections produced on the master independently, ensuring uniformity and precision across the design to achieve the stringent requirements of AR waveguide masters.

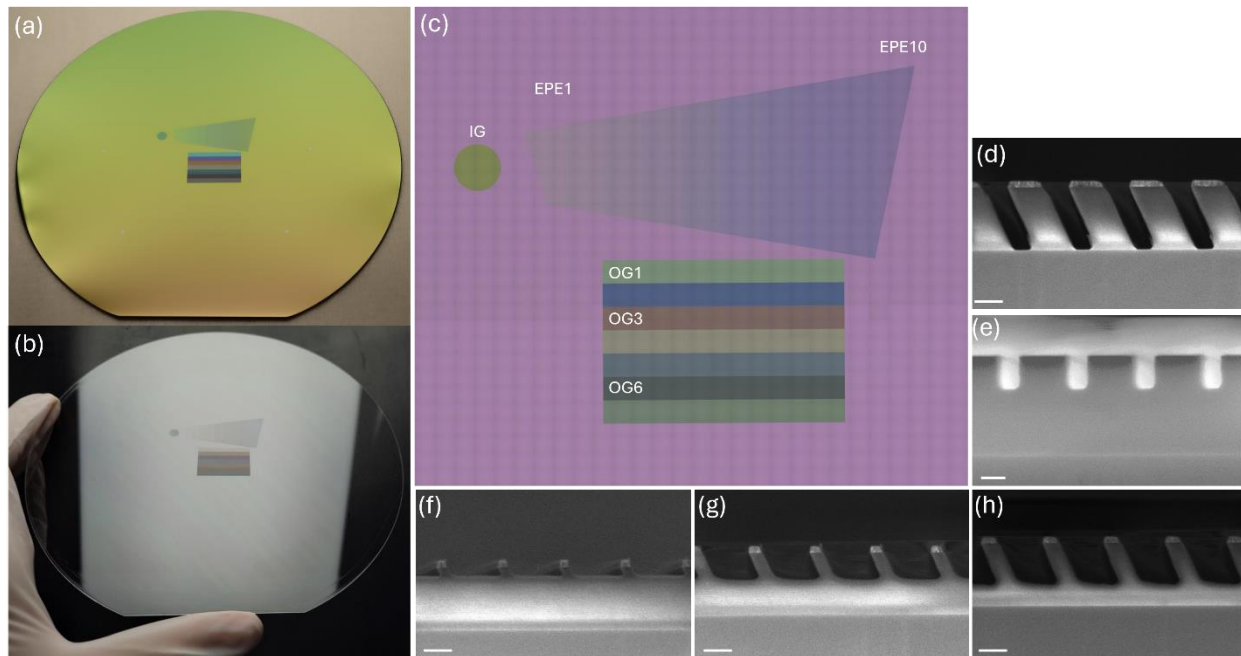


Figure 2 (a) Camera image of the 6-inch SiO₂ master, (b) camera image of a second-generation working master produced from the master in (a), (c) stitched automated microscope images of the master taken with a 5x objective. The output grating (OC) consists of sections with increasing depth and filling fraction from OG1 to OG7, while the expander grating (EPE) is composed of sections with increasing depth and decreasing filling fraction from EPE1 to EPE10, (d) cross-section SEM image of IC monitor chip (scale bar 200 nm), (e) representative cross-section SEM image of binary gratings corresponding to EPE10 in (c) (scale bar 100 nm), (f-h) xSEM images of OG1, OG3 and OG6. (scale bar 200 nm). In (d-h) the hard mask has not been removed.

2.3 Glass substrates (SCHOTT)

Specialty-grade high-index optical glass with an extremely precise surface finish forms the core of AR waveguides. SCHOTT's RealView series offers a versatile portfolio of materials and wafers with refractive indices of up to 2.0 and wafer formats up to 300mm in both round and square geometries.

Lowest wafer flatness is crucial for waveguide performance as beam path deflections caused by surface irregularities contribute to the degradation of image quality. Flatness is typically determined by the total thickness variation (TTV), with values below 1 μm being a common standard requirement in the AR industry. Achieving such low TTV values becomes increasingly challenging for large substrate sizes, yet SCHOTT has successfully established these specifications for large-area wafers.

A key goal for next-generation devices is weight saving. If substrate thickness is reduced, this means a relatively higher number of bounces of the light beam through the waveguide demanding even tighter flatness control. While TTV remains a valuable indicator of wafer flatness, localized flatness issues on the “die level”, in terms of a local wedge, become more significant. The goal is to avoid the accumulation of beam path aberrations, which directly correlate to image quality and Modulation Transfer Function (MTF) Figure 3 illustrates this relationship.

To address these challenges, an Ultra grade product line featuring significantly reduced TTV and local wedge values is available across the entire RealView portfolio. Unlike typical wafers with a slight dome shape, Ultra grade wafers maintain an ultraflat profile throughout the whole quality area, ensuring superior optical performance for advanced AR waveguides.

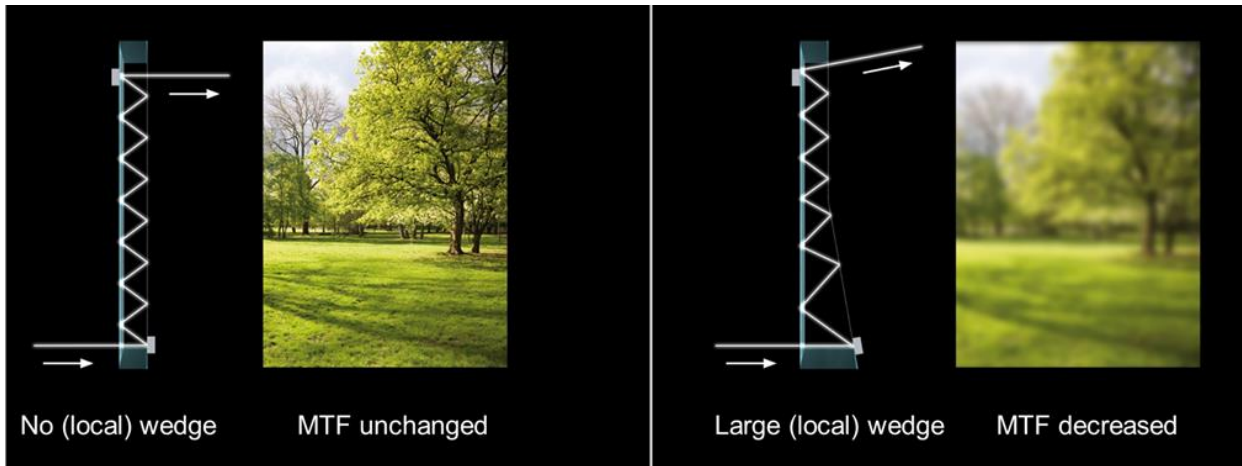


Figure 3 Lower local wedge corresponds to higher MTF values.

The strong drive for weight loss is also pushing the envelope of material innovation with a focus on the lowest density and highest refractive index. In general terms, there are opposing trends for the optimization of these two key properties, and the maximum output format might be lower. In this context, the Roll-to-Plate NIL approach for multiple wafers offers a powerful alternative for the high-volume production of next-generation AR devices when physical limitations prevent the utilization of larger sheets.

2.4 High refractive index resins (Pixelligent)

Precise replication of SRG’s is critical for the performance of AR waveguides, as they directly influence key optical properties such as diffraction efficiency and image clarity. Achieving accurate and consistent replication of these nanostructures across large areas is essential for maintaining uniform optical performance in high-volume production. The ability to achieve low Residual Layer Thickness (RLT) and consistent structural fidelity enables improved waveguide efficiency, minimal optical aberrations, and superior MTF.

Pixelligent’s PixNIL® SFT1 and PixNIL® ST16, both UV-curable titania-polymer nanocomposites, were employed to fabricate high-quality SRGs for AR waveguides using NIL. Specifically designed to meet the stringent optical and structural requirements of advanced AR devices, these resins deliver high refractive indices, low RLT, and structural integrity, ensuring precise replication of complex grating geometries across a wide process window. PixNIL® resins offer high transparency solutions with <0.1% haze, attributed to the tight control over particle size, shape, and surface of the proprietary PixClear® nanocrystals, as shown in Figure 4. This results in high optical clarity and minimal scattering, both of which are essential for maintaining image quality in AR waveguides.

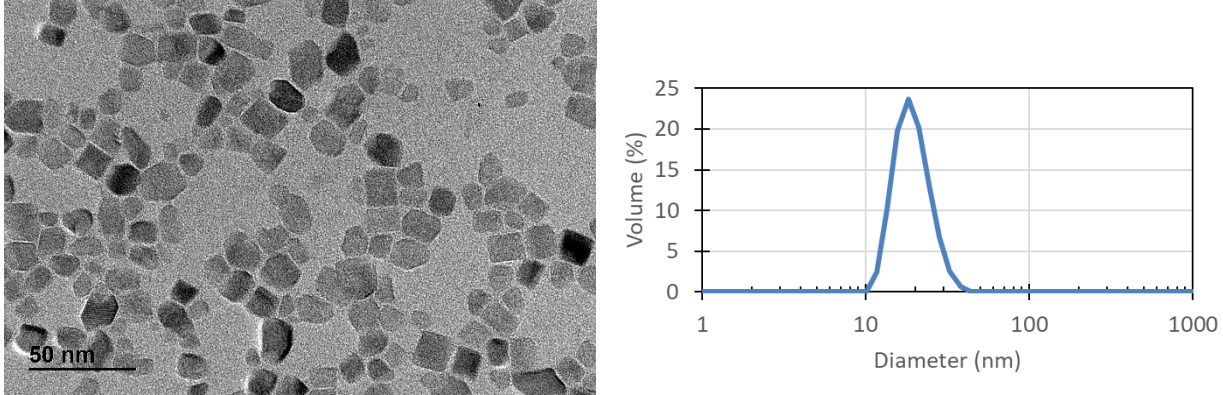


Figure 4 (left) TEM image of titania nanocrystals deposited from a dispersion onto a TEM grid (right) typical DLS curve of titania nanocrystals, illustrating the narrow size distribution.

PixNIL® SFT1 is a solvent-free formulation with a refractive index of 1.86 at 589 nm wavelength and a viscosity of approximately 500 cP. Its solvent-free composition ensures straightforward processing and deposition uniformity, advantageous for imprinting. PixNIL® ST16, in contrast, is a solvent-containing formulation designed to achieve thin film thicknesses (< 1 μm) and low RLTs (<30nm) with a refractive index of 1.83 at 589 nm wavelength. This resin shows excellent compatibility with various stamp materials (e.g. silicone, acrylic) enhancing its versatility, and ensuring precise replication and high-quality imprints across diverse manufacturing setups.

2.5 Large-Area Nanoimprinting (Morphotonics)

The surface relief gratings of the AR waveguide can be replicated from the working master into high refractive index material using NIL. The large-area R2P NIL technology of Morphotonics enables high throughput manufacturing while ensuring scalability and high replication quality. The replication of both binary and blazed SRG with high quality texture fidelity as well as in track-pitch variation, has been previously demonstrated using Morphotonics equipment [1-3]. The replication of 480 waveguides on a Gen5 imprint area (1100 mm x 1300 mm) in a single imprint cycle has been shown using Morphotonics Portis NIL1100 equipment Figure 5a) [4].

The schematic in Figure 5b) illustrates the working principle of R2P NIL. A flexible stamp carrying the inverted texture (1) is mounted on a system of four guiding rollers. A rigid substrate is coated with a UV-curable resin (2) and the flexible stamp is laminated onto it (3). The sandwiched structure of substrate, liquid resin and flexible stamp is transported by the roller system and passes under a UV source (4) which cures the resin before the flexible stamp is delaminated from the cured resin and substrate by the following roller (5).

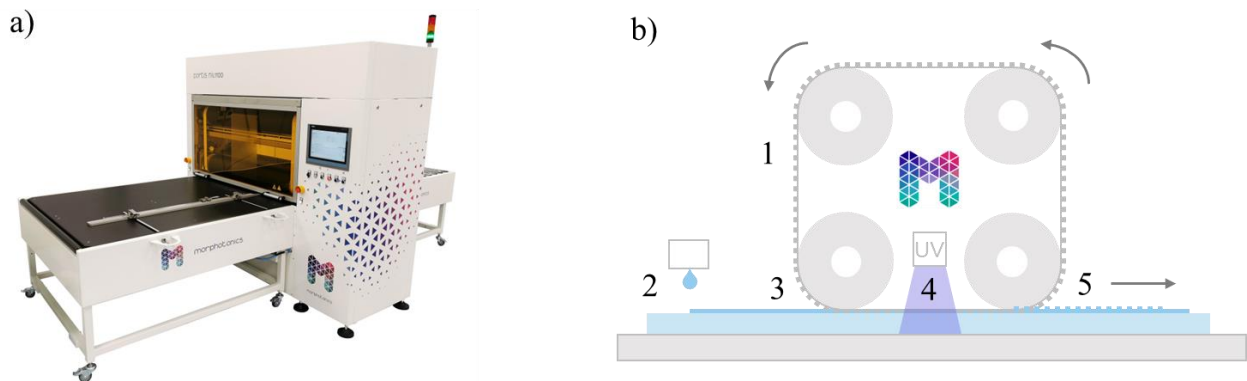


Figure 5 a) Morphotonics Portis NIL1100 nanoimprint equipment b) Schematic of R2P NIL.

The large-area capability of R2P NIL can also be exploited to imprint multiple smaller substrates in a single imprint cycle by using a wafer carrier. A wafer carrier is a transport plate containing pockets sized to fit the substrates to be imprinted. When the imprint substrates are placed in the pockets, a uniform flat top-surface is achieved, allowing a uniform imprint process. This is specifically relevant for the manufacturing of AR waveguides as high refractive index substrate are typically wafer sized and imprint uniformity is key. By enabling wafer based imprinting, Morphotonics nanoimprint technology can seamlessly integrate into existing wafer-based process chains. In previous work, imprinting of nine square substrates of size 300 mm x 300 mm in a single imprint cycle has been shown [2].

To demonstrate scalability and compatibility with circular imprint substrates, five high refractive index wafers (200 mm diameter) were imprinted in a single imprint cycle using a Gen3 (550 mm x 650 mm) sized wafer carrier, as shown in the schematic in Figure 6a). To show that uniformity and high imprint quality are both maintained over the five imprint substrates as well as over multiple repeated imprints, 10 imprint cycles are performed with the same flexible stamp. On each 200 mm wafer, four AR waveguides with slanted design (Figure 1) were replicated, see an example of imprint in Figure 6b). In 10 imprint cycles, a total of 200 waveguides have been produced. The replication was done using 1.86 refractive index solvent-free resin (PixNIL® SFT1, Pixelligent) and 2.0 refractive index substrates (SCHOTT RealView®, standard and ultraflat).

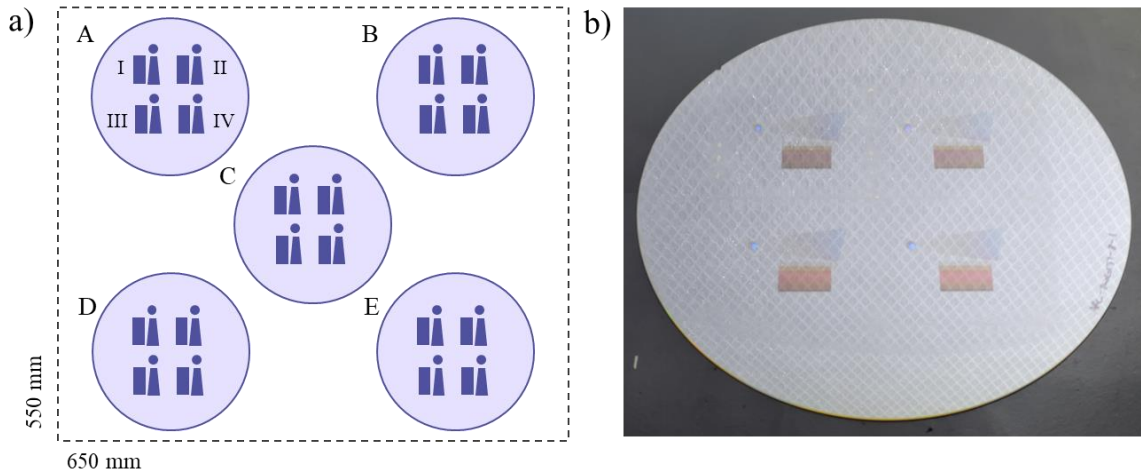


Figure 6 a) Schematic of imprint arrangement for imprinting five 200 mm wafers each containing four AR waveguides and naming of the wafer positions (A-E) and waveguide positions (I-IV), b) Imprinted wafer with four AR waveguides, 1.9 refractive index resin on 2.0 refractive index glass.

The wafer-based imprinting method demonstrated in this work can be scaled to accommodate wafer carriers as large as Gen5 (1100 mm x 1300 mm), enabling the simultaneous imprinting of up to 13 round wafers, each with a 300 mm diameter. In a single imprint cycle, this setup has the potential to produce 299 waveguides (23 waveguides per wafer). Similarly, for square wafers (300 mm x 300 mm), up to 12 square wafers can be processed in a single cycle, producing 480 waveguides (30 per wafer) as illustrated in Figure 7.

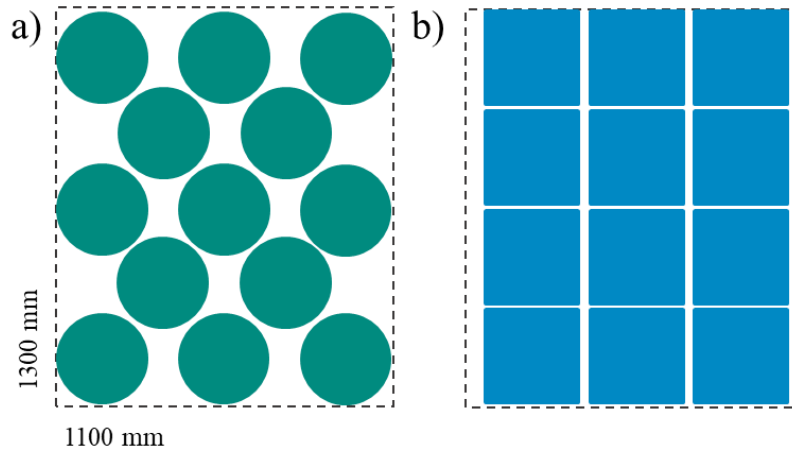


Figure 7 a) Schematic of 13 x 300 mm round wafers on 1100x1300mm Gen5 area, b) Schematic of 12 x 300 mm square wafers on 1100x1300mm Gen5 area.

While standard Morphotonics technology is based on solvent-free resins, the nanoimprint equipment and material is also compatible with solvent-containing resins. By applying those resins through spin coating and subsequent imprinting using R2P NIL, AR waveguide imprints with low RLT can be produced [3]. To further demonstrate compatibility of a slanted AR waveguide design with spin-coatable (solvent containing) resins and achieve thin RLT (<400 nm), 12 single wafer imprint cycles were conducted. Four AR waveguides were imprinted on each wafer using a 1.83 refractive index solvent-containing resin (PixNIL® ST16, Pixelligent) and 2.0 refractive index substrates (SCHOTT RealView®, standard and ultraflat).

2.6 Waveguide singulation (3D-Micromac)

In order to have a reliable and scalable solution for cost-effective AR waveguide manufacturing from lab scale to mass production, the singulation of the eyepieces plays an essential role. 3D-Micromac optimized its laser cutting process specifically for high refractive index substrates used to produce AR eyepieces, ensuring high yield and precision. The equipment used is based on laser modification cutting, a recognized production process in the display industry known for its ability to produce high-quality cuts with minimal edge defects. The process flow of this cutting process is illustrated in Figure 8a). First, the glass (filamentation) is modified along a pre-determined curve (the intended break line) and through the entire material thickness using pico- or femtosecond laser pulses. Each point of modification is created by the local impact of a single laser pulse or pulse bursts. Then, a secondary process step is required to separate the glass along the break line. For free-form geometries, the required stress is typically introduced by exposing the modification and its surrounding material to a CO₂ laser [5].

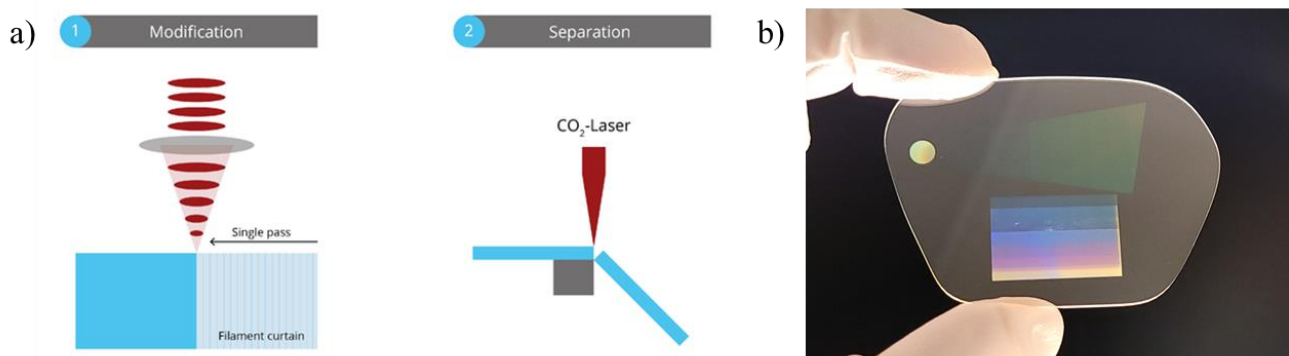


Figure 8 a) Laser cutting process flow, image extracted of reference [5]. b) Picture of cut eyepiece produced for this work.

This technique was previously validated, showing that the 4 point bending strength of the glass was strengthened by more than 48% (equal on laser exit and entrance side) when using the optimized laser modification process [5]. 3D-Micromac's results are proven to be stable and mass-production ready.

Building on these proven results, 3D-Micromac developed the microPOLAR system- a modular, field-upgradable solution tailored for the AR market. It can process bare wafers or wafers applied on adhesive tape. Additionally, the system's base is an industrial-proven and mature transport system that offers the possibility to integrate different processes, handling and quality inspection modules to provide users with a high degree of flexibility. This modularity ensures adaptability to different product designs and production requirements, while maintaining competitive cost per piece values. Figure 8b) shows an example of a cut eye-piece produced using the high refractive index materials and R2P NIL described in this manuscript.

The high quality singulated eyepieces produced through this process were used in the demonstrator produced as a result of this work. This cutting-edge approach ensures precision, scalability, and cost-effectiveness, making it a key enabler for the production of next-generation AR devices.

2.7 Metrology (OptoFidelity)

The AR waveguides produced in this work were characterized using two test systems: one for measuring grating quality (grating pitch and angle) and the other for gauging the image quality performance of the waveguides. Figure 9 shows the two systems used.

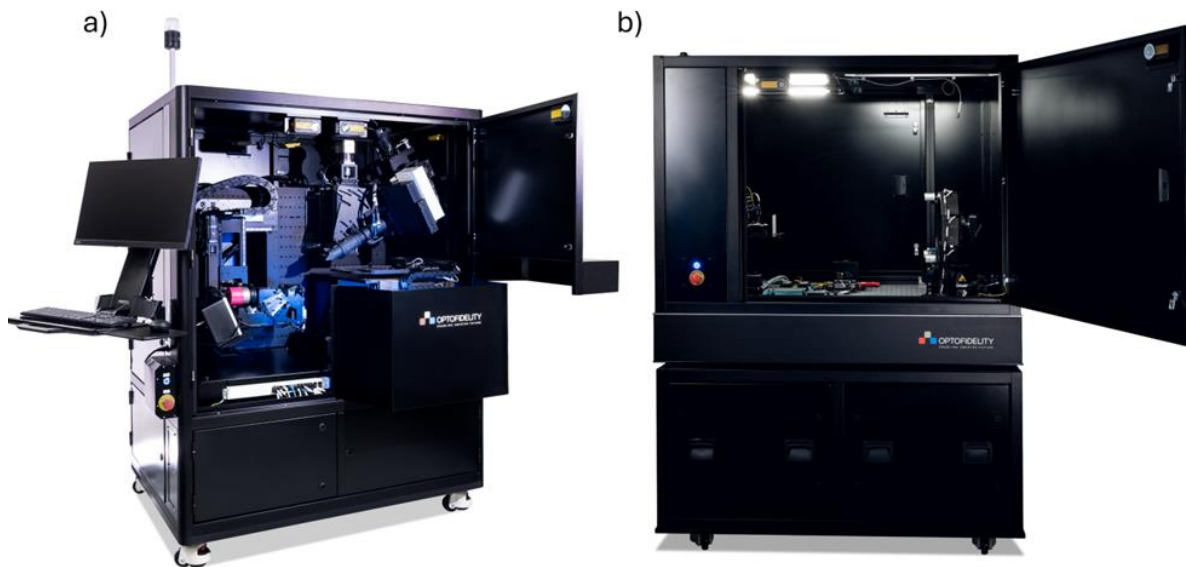


Figure 9 a) OptoFidelity WG-IQ, b) OptoFidelity WG-GAT.

WG-GAT is a Littrow diffractometer with a motorized sample holder and a laser beam scanner, achieving sub-picometer pitch resolution and arcsecond angle resolution. With a 1 mm diameter, 405 nm laser beam it can scan AR waveguides to detect non-uniformities in grating pitch and angle across the surface. This high-resolution capability ensures that any deviations from design specifications are accurately measured and provides critical insights into changes across multiple imprint cycles, which is critical for maintaining consistent optical performance over large-scale production.

WG-IQ utilizes an optical replica of a human eye to analyze AR waveguide image quality metrics. The combination of state-of-the-art optical instruments and robotics ensures accurate and automated sample handling and alignment critical for repeatable and reliable measurements. Figure 10 presents example results from both WG-IQ and WG-GAT systems.

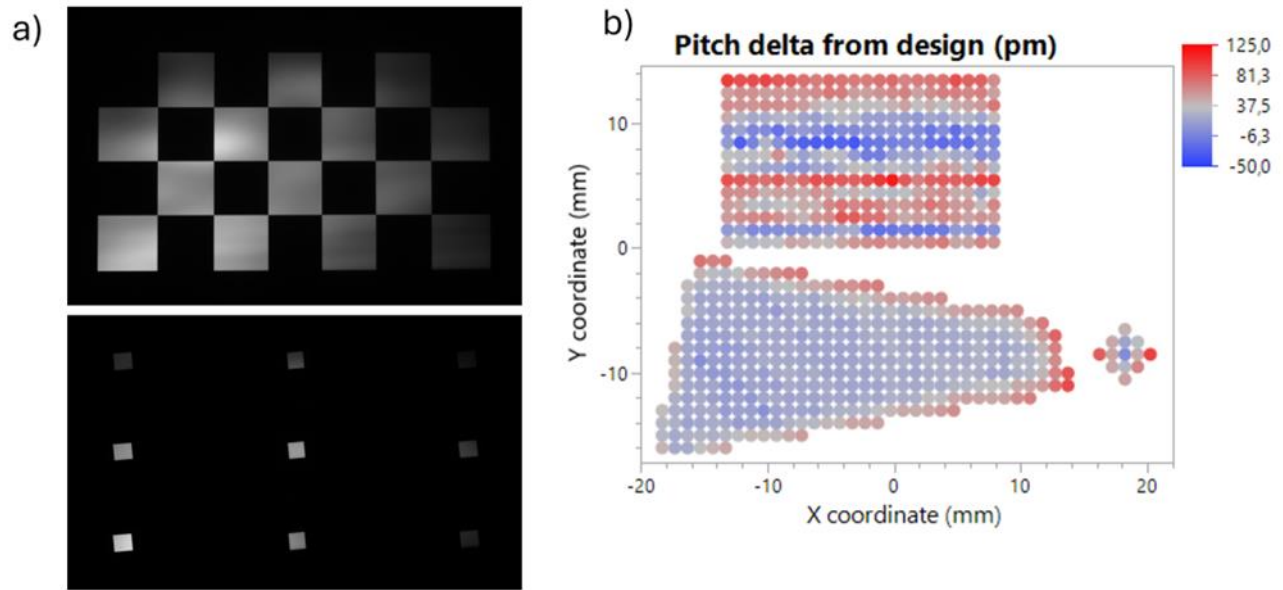


Figure 10 a) Example result of measurement images taken with WG-IQ, b) example result of pitch measurement of an AR waveguide submaster with WG-GAT system.

When characterizing AR waveguides, it is important to choose relevant and standardized metrics to gauge the performance of the samples. With WG-GAT, grating pitch non-uniformity, grating angle non-uniformity as well as average grating pitch and angle compared to design pitch and angle were used in grading the samples. On the image quality side, average vertical and horizontal MTF at 13 cycles per degree were chosen as key metrics.

These metrology results provide critical validation of the waveguide fabrication process, ensuring that the replicated gratings and overall optical performance meet the stringent requirements for next-generation AR devices.

3. RESULTS

3.1 Mastering

The ridge widths (measured at half depth) on the master for the IC, OC and EPE are within $\pm 0.4\%$, -3.6% to $+6.5\%$ and $+1.5\%$ to $+2.4\%$ of the target values, respectively. The etch-depth of the gratings on the master is pre-compensated to account for 6% material shrinkage from master to 2nd generation working master that is used for further replications. The measured grating depths on the master are within $\pm 1\%$, -5.2% to $+2.3\%$ and -0.4% to $+4.5\%$ of the target depths for IC, OC and EPE, respectively.

The tapering angles of the slanted gratings for IC and OC are measured to be within $\pm 0.5^\circ$ and 1.5° to 6.5° of the target angle 24.9° . These small deviations are considered acceptable and ensure that the desired performance range is achieved. Overall, these results demonstrate that the fabricated master grating meets the necessary dimensional accuracy and structural fidelity required for high-quality replication in subsequent manufacturing steps.

3.2 Imprint quality

In Figure 11 TEM images of the IC grating from waveguides imprinted with PixNIL® SFT1 and PixNIL® ST16 resins are shown. From Figure 11a) and Figure 11b) it can be seen that with both formulations a good nanoparticle dispersion is achieved throughout the slanted grating. This consistent nanoparticle distribution is critical for minimizing light scattering and ensuring uniform optical properties across the waveguide. Figure 11c) reveals a low residual layer thickness of around 210 nm underneath the IC grating obtained with the solvent-containing resin PixNIL® ST16. Achieving low RLT is important for improving diffraction efficiency and minimizing waveguide propagation losses. Further optimization of RLT was beyond the scope of this study. Overall, the imprint quality was high, with well-defined grating features and uniform nanoparticle dispersion across the structures. These results demonstrate the material compatibility of both solvent-free and solvent-containing resins with the imprinting process, validating their suitability for large-scale AR waveguide production.

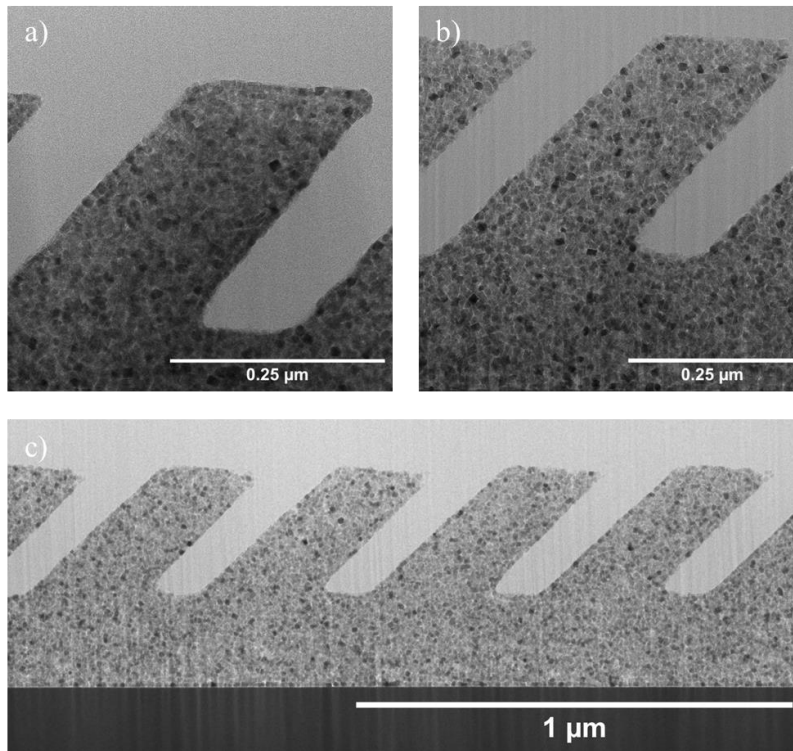


Figure 11 a) TEM image of IC grating made of PixNIL® SFT1, imprint cycle 1, b) TEM image of IC grating made of PixNIL® ST16, imprint cycle 2, c) TEM image of IC grating made of PixNIL® ST16, imprint cycle 12 with the glass substrate being visible revealing the residual layer thickness.

3.3 Grating quality

The measured samples and their parameters are shown in Table 1. Each sample has a unique sample identifier (*ID*). The *Cycle* column indicates the manufacturing/imprint cycle, while the *wafer* column marks the wafer position in each manufacturing cycle. The *waveguide* column marks the waveguide position in each wafer (see naming convention Figure 6). The used materials are described with *glass type* which differentiates between dome-shaped and ultraflat substrates and *resin*, which marks the used imprint resin type.

Table 1 Overview of the waveguides used for Littrow diffractometry and image quality measurements. The samples are referred to using the sample identifier (ID). Manufacturing characteristics as cycle, wafer, waveguide, glass type and resin for each measured sample are described. For single wafer imprinting no wafer position is specified.

ID	Cycle	Wafer	Wave-guide	Glass type	Resin	ID	Cycle	Wafer	Wave-guide	Glass type	Resin
1AIII	1	A	III	Ultraflat	SFT1	2DIII	2	D	III	Dome	SFT1
1BIII	1	B	III	Ultraflat	SFT1	2EIII	2	E	III	Dome	SFT1
1CI	1	C	I	Ultraflat	SFT1	10AIII	10	A	III	Ultraflat	SFT1
1CII	1	C	II	Ultraflat	SFT1	10BIII	10	B	III	Ultraflat	SFT1
1CIII	1	C	III	Ultraflat	SFT1	10CI	10	C	I	Ultraflat	SFT1
1CIV	1	C	IV	Ultraflat	SFT1	10CII	10	C	II	Ultraflat	SFT1
1DIII	1	D	III	Ultraflat	SFT1	10CIII	10	C	III	Ultraflat	SFT1
1EIII	1	E	III	Ultraflat	SFT1	10CIV	10	C	IV	Ultraflat	SFT1
2AIII	2	A	III	Dome	SFT1	10DIII	10	D	III	Ultraflat	SFT1
2BIII	2	B	III	Dome	SFT1	10EIII	10	E	III	Ultraflat	SFT1
2CI	2	C	I	Dome	SFT1	1IV	1		IV	Ultraflat	ST16
2CII	2	C	II	Dome	SFT1	3IV	3		IV	Ultraflat	ST16
2CIII	2	C	III	Dome	SFT1	8IV	8		IV	Ultraflat	ST16
2CIV	2	C	IV	Dome	SFT1	10IV	10		IV	Dome	ST16

The samples presented in Table 1 were selected to study manufacturing stability between different cycles, wafer locations and waveguide locations, and to study the effect of glass type and HRI resin on image quality. Four samples (1IV, 3IV, 8IV and 10IV) were manufactured with a solvent containing resin applied by spin coating to achieve low RLT. While the effects of low RLT and refractive index cannot be perfectly decoupled, these samples provide valuable insights into how thin RLT layers influence grating quality and image clarity.

Grating pitch and angle non-uniformities were measured using WG-GAT tool with a 1 mm diameter laser beam. The tool captured data from 49 measurement points for EPE gratings, 10 points for IC gratings and 51 points for OC gratings. Non-uniformities were calculated for each sample as standard deviation of all measurements from a given grating. Figure 12 presents the grating quality results from cycle 1 samples.

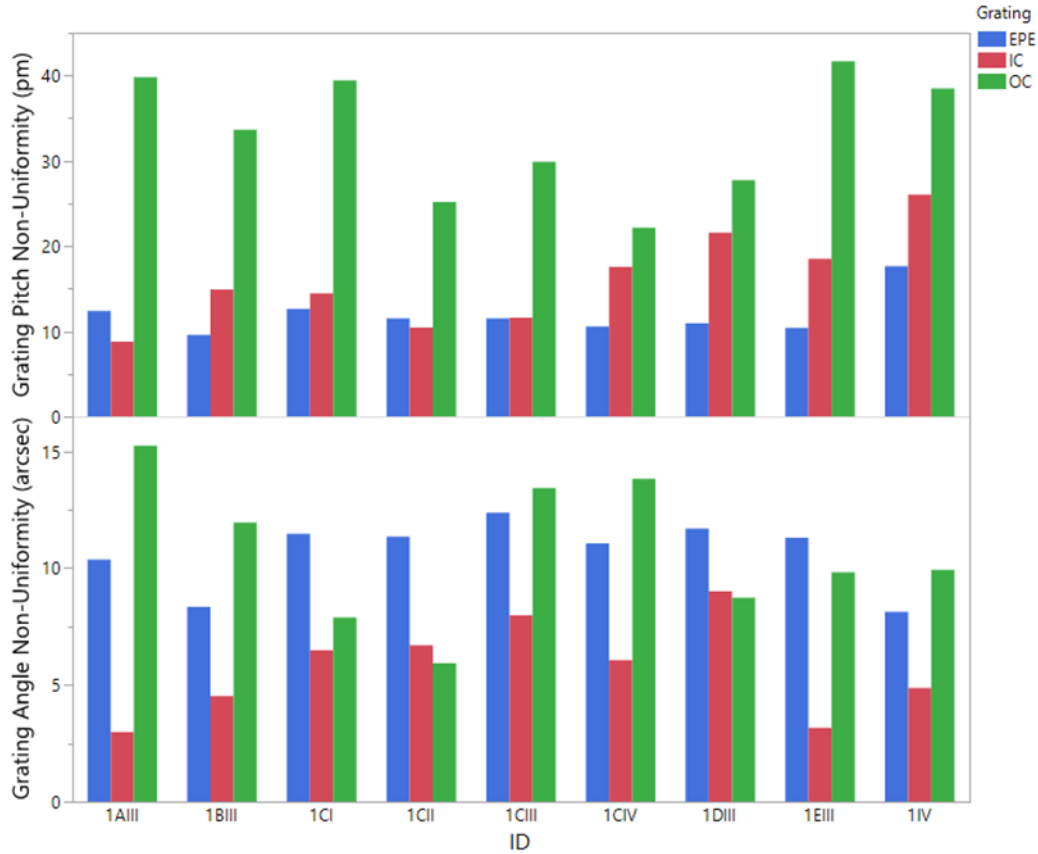


Figure 12 WG-GAT grating parameter comparison between different wafers and waveguides from the first manufacturing cycle. Grating angle non-uniformity and grating pitch non-uniformity are shown for each grating (EPE, IC, OC) separately. Results indicate good overall uniformity and manufacturing stability between different wafers and waveguides.

Results from Figure 12 demonstrate overall good non-uniformities values for grating pitch and angle. The data shows no significant differences in pitch and angle non-uniformities between different wafers and waveguides within one imprint cycle. Similar grating quality is achieved with both imprint resins (PixNIL® SFT1 and PixNIL® ST16). However, there is a visible trend of worse quality in OC compared to IC and EPE gratings, but this trend is not as evident in angle non-uniformity as it is in pitch non-uniformity.

Another research objective was to determine if the grating quality changes between different manufacturing cycles. Figure 13 presents measurement data comparing grating quality between cycle 1 and cycle 10. Results are further separated into different wafers and grating type, but same samples with same waveguide quality are compared for the sake of visualization.

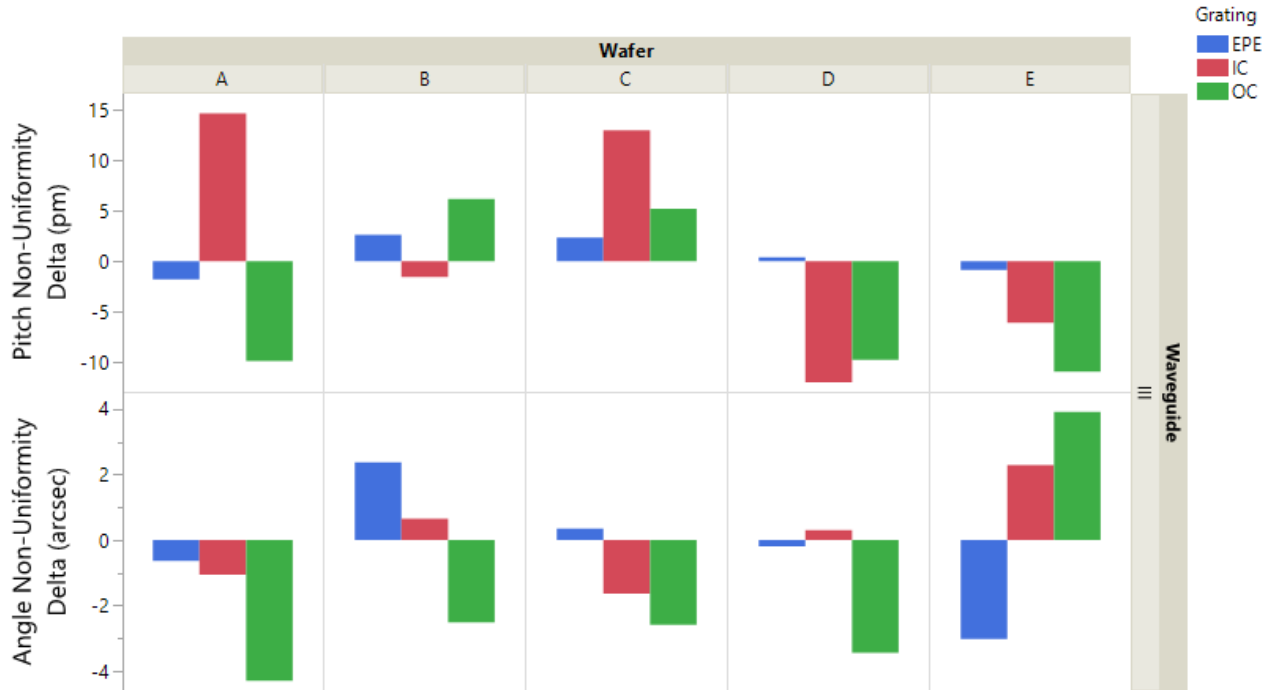


Figure 13 WG-GAT grating parameter comparison between manufacturing cycles 1 and 10. Positive value means that the measured parameter grew from cycle 1 to cycle 10 while negative value means that the respective parameter decreased from cycle 1 to cycle 10. Grating angle non-uniformity and grating pitch non-uniformity are shown for each grating (EPE, IC, OC) separately. Results are taken from each wafer while comparing only samples with same waveguide location (III), same glass type (ultraflat) and same resin type (PixNIL® SFT1).

Results from Figure 13 show that there are no major differences in grating quality between different manufacturing cycles. The variation of grating quality between different samples is typically larger than the variation caused by differences in manufacturing cycles. These findings validate the stability of the NIL process across multiple cycles, indicating its suitability for high-volume production of AR waveguides with consistent optical performance.

3.4 Image quality

Image quality measurements for the sample were performed with WG-IQ tool. Although many metrics can be used to quantify image quality, this work focuses on average horizontal and vertical MTF at 13 cycles/degree. This metric combines resolution and contrast while characterizing the performance at different field points, providing a comprehensive measure of waveguide image quality when averaged over several measurement locations. Figure 14 presents average horizontal MTF results from each sample.

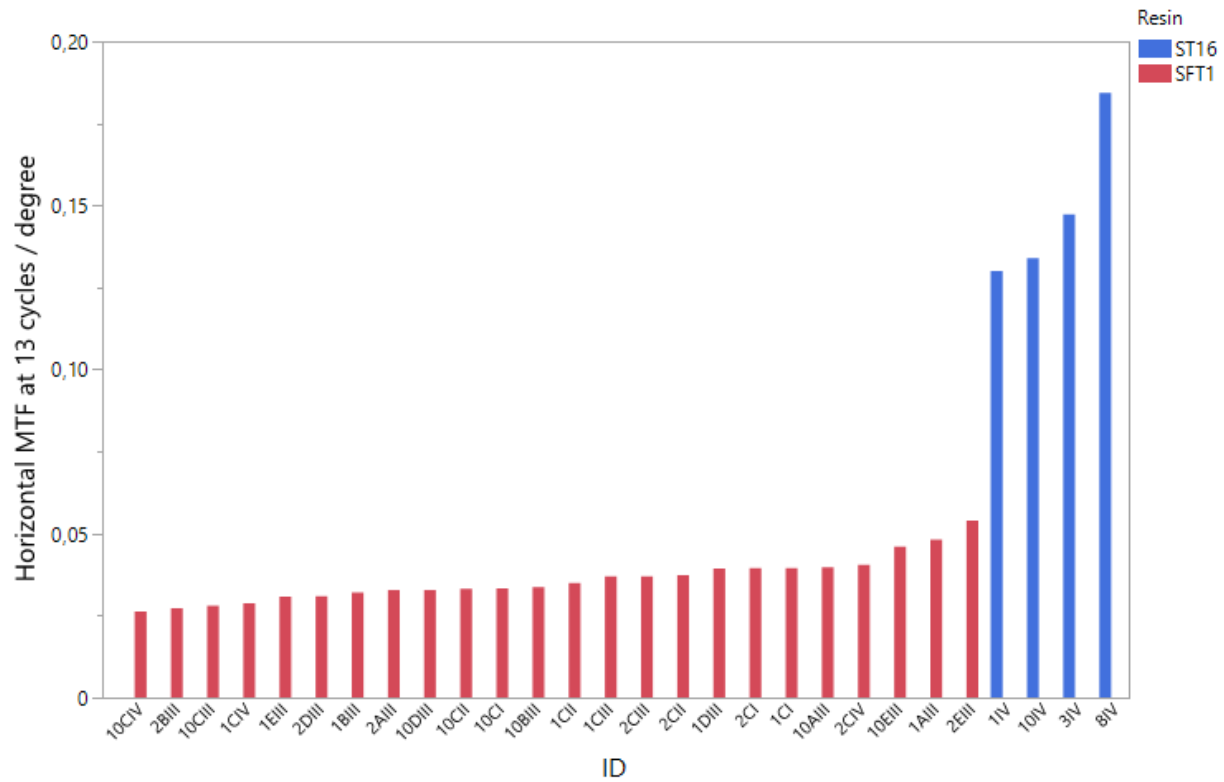


Figure 14 Image quality results from all measured samples. All measurements were performed with green light in the same eye-box location.

From Figure 14, it is evident that there is a large difference in MTF between the two resins. Both resins exhibit similar refractive index and replication quality, the main difference lies in the residual layer thickness which is 4.5 μm for solvent free resin PixNIL® SFT1 and <400 nm for solvent containing resin PixNIL® ST16. The improved MTF for imprints with low RLT could be attributed to optical aberrations from the interaction between light and the buffer region between the gratings and the substrate for imprints with excessive thickness.

The same results can also be used to compare differences between manufacturing cycles and the effects of waveguide and wafer locations. These comparisons are presented in Figure 15.



Figure 15 Image quality results from all measured samples with STF1 resin. All measurements were performed with green light in the same eye-box location.

Results of Figure 15 demonstrate that there is no significant difference in image quality between different waveguide or wafer locations, nor is there a significant difference in image quality caused by the manufacturing cycle. This consistency further validates the stability of the manufacturing process.

Finally, potential improvements in image quality coming from using ultraflat glass instead of domed glass were investigated. As shown in Figure 14, samples produced with PixNIL® SFT1 on ultraflat glass (cycles 1 and 10) did not have a significantly different MTF performance compared to samples with domed glass (cycle 2). However, there is evidence of improvements to be seen when comparing samples with PixNIL® ST16 resin shown in Figure 16.

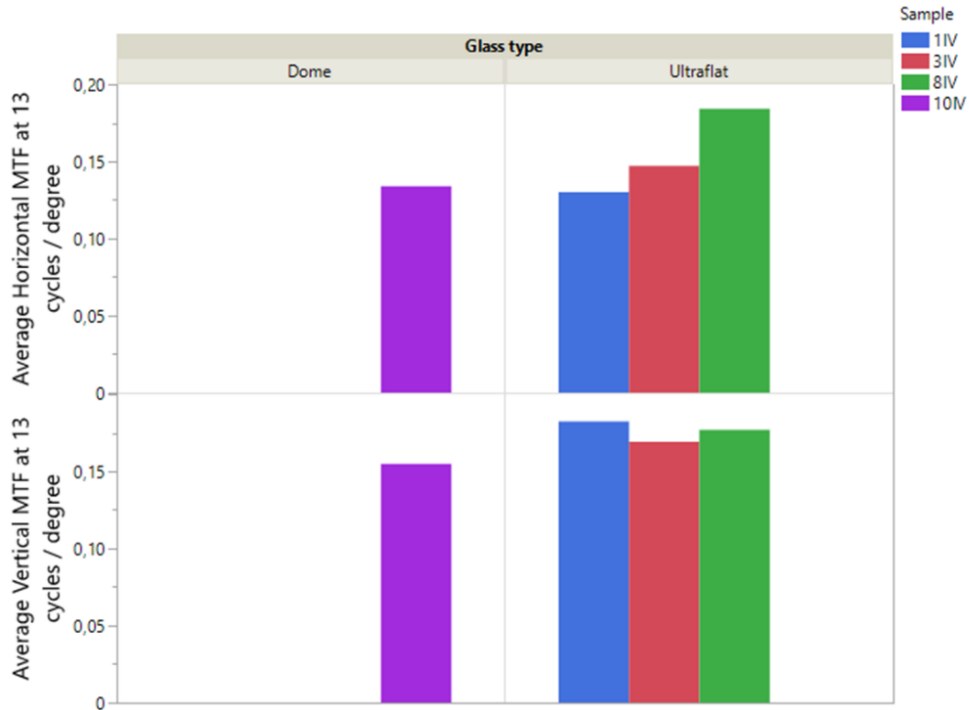


Figure 16 Image quality results from all measured samples with PixNIL® ST16 resin. All measurements were performed with green light in the same eye-box location.

Figure 16 demonstrated that there are possible improvements to MTF when using ultraflat glass instead of domed glass. The reason why glass type appears to influence MTF (primarily with PixNIL® ST16) could be due to differences in residual layer thicknesses between different resin types. Meaning, low TTV of the substrate becomes more relevant the thinner the residual layer thickness of the imprint layer is. It is also possible that glass type affects other image quality performance metrics than MTF. Additionally, the number of samples with PixNIL® ST16 resin was limited to only 4 samples, hence the glass type results with these samples should be taken with caution. A more pronounced MTF improvement is expected when using ultraflat glass for thoroughly optimized, state-of-the-art waveguides with reduced thickness, where flatness becomes a more significant bottleneck for MTF.

4. CONCLUSION

In this work, the comprehensive integration of the full process chain of AR waveguide manufacturing has been successfully demonstrated; from design, materials, mastering, large area imprinting, singulation and performance testing. A novel approach for mass manufacturing via multiple wafer imprinting using round glass substrates with large-area NIL has been exemplified, highlighting its scalability and compatibility with wafer-based processing.

A complex AR waveguide design featuring slanted gratings was uniformly replicated across multiple wafers and imprint cycles, maintaining consistent grating fidelity and high image quality of the final waveguides. The demonstrated process accommodates a variety of materials, including high RI resins, both solvent-free as well as solvent-containing to achieve low residual layer thickness, and next generation ultraflat high RI glass substrates. This material versatility demonstrates compatibility with diverse design requirements and manufacturing conditions.

This work underscores the transformative potential of large-area NIL in the AR industry by addressing key challenges in cost-efficiency and production scalability. With the demonstrated advancements in material compatibility, image quality performance, and wafer-handling techniques, this approach significantly contributes to the path toward widespread adoption of AR smart glasses, paving the way for the next generation of immersive technologies.

ACKNOWLEDGMENTS

The authors would like to thank their colleagues for their support on this work, with special thanks to Ievgen Kurylo, Lotje Jobse and Niels Dalmijn from Morphotonics B.V. and Jonny Lippmann and René Liebers from 3D-Micromac AG. Funded by the European Union. Views and opinions expressed are however those of the author(s) only and do not necessarily reflect those of the European Union or European Innovation Council and SMEs Executive Agency (EISMEA). Neither the European Union nor the granting authority can be held responsible for them.

REFERENCES

- [1] M. Jotz et al., “The path towards mass manufacturing of optical waveguide combiners via large-area nano-imprinting,” Proc. SPIE 11931, 1193109 (2022).
- [2] S. Steiner et al., “Enabling the Metaverse through mass manufacturing of industry-standard optical waveguide combiners,” Proc. SPIE 12449, 1244906 (2023).
- [3] S. Steiner et al., “Exploring the boundaries of large-area nanoimprinting for mass production of AR waveguides” Proc. SPIE 12913, 129131D (2024).
- [4] M. Ballottin et al., “Practical considerations for large-area nanoimprinted augmented reality waveguides” Proc. SPIE 12957, 129570J (2024).
- [5] M. Jotz et al., “High strength laser cutting of high refractive index wafers for augmented reality” Proc. SPIE 12449, 124491U (2023).